JMEPEG (2004) 13:413-420
DOI: 10.1361/10599490419964

1059-9495/$19.00

Electrochemical Planarization of Patterned Copper Films for Microelectronic Applications

J. Huo, R. Solanki, and J. McAndrew

(Submitted February 10, 2004)

Electrochemical polishing (ECP) of copper (Cu) using solutions of phosphoric acid, sulfuric acid, sodium chloride, ethylene glycol, and hydroxyethylidenediphosphonic acid (HEDP), with or without organic and inorganic additives, has been investigated as an alternative to chemical mechanical polishing (CMP) for integration of low-k dielectrics in microelectronic devices. Copper anodic polarization curves in these solutions were measured. ECP of Cu bulk and thin films in these solutions was evaluated with atomic force microscopy and scanning electron microscopy. It was shown that most of the solutions studied have polarization curves with a limiting current plateau characteristic of ECP. Among them, phosphoric acid, HEDP, and phosphoric acid solutions with ethylene glycol, sodium tripolyphosphate, and Cu oxide as additives produced the best electropolished surfaces (mean roughness: R_a < 10 nm) on bulk Cu. However, satisfactory ECP of electroplated patterned Cu films on silicon wafers were achieved only with an electrolyte that produced a salt film at the anode surface. Based on these experimental results, ECP mechanisms and optimal conditions for ECP of patterned Cu films plated on silicon wafers are presented.

Keywords chemical mechanical polishing (CMP), electrochemical planarization, Cu, Cu film, Cu interconnect, electrochemical polishing (ECP), electropolishing, electropolishing mechanism, polarization curve

1. Introduction

Damascene is the most common technique used for fabricating copper (Cu) interconnects in microelectronic devices. In this method, Cu is first electroplated to fill vias and trenches in an interlayer dielectric (ILD). The excess Cu is then removed using chemical mechanical polishing (CMP), leaving the recessed structures filled with Cu. To increase device speed, it is necessary to reduce the capacitance between interconnects and, thus, reduce resistance capacitance (RC) delay. For this purpose, a lower dielectric constant ILD is required. To further reduce the dielectric constant, porosity can be introduced into the films. Unfortunately, these low-k ILDs are too soft to be easily integrated with CMP, and future porous materials will be even more difficult. Hence, alternate polishing techniques are urgently needed. One possible solution is electrochemical polishing/planarization (ECP).

ECP is a mature technology that has been used for surface polishing of bulk metal materials such as Cu and stainless steel. However, it is a new application in microelectronic fabrication. Bulk Cu and Cu films electrodeposited on deep trenched silicon wafers have different surface characteristics. A previous study[1] showed that it is much more challenging to planarize the gently undulating surface of Cu films electroplated on patterned wafers than to planarize bulk Cu surface. ECP effects strongly depend on anodic layers and their surface profile, limiting current and potentials, and mass transport control species. These factors are mainly determined by electrolytes and their concentrations in the solution. At present, phosphoric acid is the most commonly used electrolyte. However, satisfactory ECP effects of Cu films electroplated on patterned wafers was not achieved with the phosphoric acid solution.

It is known that electropolishing can be achieved only in the range of the limiting current plateau of a current-potential (polarization) curve under mass transport control.[2] Therefore, to search for ECP electrolytes and for favorable experimental conditions, this investigation started with the determination of Cu anodic polarization curves of various electrolyte solutions. Then ECP of bulk Cu and thin films in these solutions were evaluated, and possible mechanisms discussed. Finally, the optimal conditions for ECP of Cu films electroplated on patterned silicon wafers are presented.

This paper was presented at the 2nd International Surface Engineering Congress sponsored by ASM International, on September 15-17, 2003, in Indianapolis, Indiana, and appears on pp. 389-97 of the Proceedings.

J. Huo and **J. McAndrew,** Electronics R&D Group, Air Liquide, Countryside, IL; and **R. Solanki,** OGI School of Science and Engineering, OHSU, Beaverton, OR. Contact e-mail: jinshan.huo@airliquide.com.

2. Experimental Details

2.1 Measurement of Polarization Curves

Copper anodic polarization curves were measured using linear sweep voltammetry (LSV) under computer control with a 273A Potentiostat/Galvanostat (Princeton Applied Research, Oak Ridge, TN). The voltage scan range was 0-4 V, and the scan rate was 5 mA/s. The speed of rotating disk was 100 rpm. The distance between working and counter electrodes was about 15 mm. A customized rotating-disk electrode with Cu disks was used as the working electrode. The Cu disks were 11.3 mm in diameter (1 cm^2) with a thickness of 1.5 mm. The Cu samples were hand polished with 1 μm slurry and cleaned with acetone before the LSV experiments. The counter electrode consisted of a Cu plate 12 mm thick and 43 mm in diameter. The reference electrode used was Ag/AgCl in 3 *M* KCl. A Teflon cylinder, with an acid resistant filter at the

bottom, was used to prevent the hydrogen bubbles (i.e., bubbles formed on the counter electrode) from reaching the anode (working electrode) surface. All experiments were carried out in a 200 mL glass container with 100 mL solution at room temperature. The electrolyte solutions studied are listed in Table 1.

2.2 Electrochemical Polishing

ECP of Cu disks was performed using computer-controlled chronoamperometry (CA). Sample preparation was the same as that used for polarization curve measurements. ECP of Cu films on patterned silicon wafers was performed in the same system, except a customized sample holder was used to hold the 5 × 5 cm wafers in a larger cylindrical container (about 3 L in volume). In addition, a conical filter was used to block any hydrogen bubbles from reaching the anode surface. The wafer coupons for ECP were cut from 200 mm diameter deep-trenched wafers, on which Cu films had been electroplated beforehand with OGI's in-house wafer plating system. The controlled potentials for ECP were the middle points of the limiting current plateau on the polarization curves. All the experiments were performed at a 100 rpm anode rotating speed and at room temperature.

Surface profiles of the samples before and after ECP were investigated using atomic force microscopy (AFM), optical microscopy, and electron microscopy, as well as a surface profilometry. For each sample, three AFM images were taken and the average of the roughness (R_a) was determined. The polishing (or removal) rate R_d was calculated from the weight of the samples measured before and after electropolishing and compared with the calculated values determined from the polishing current. Electrolyte solutions were prepared by volume, using commercially available solutions with wt.% as given in the footnote of Table 1.

3. Results and Discussion

3.1 Limiting Current Data of Copper Anodic Polarization

A typical polarization curve is shown in Fig. 1. Limiting current (i_L) and potential range (E_L) of the limiting current plateaus were obtained from the measured polarization curves.

Table 1 Electrolyte Solutions Used for Polarization Curve Measurements

Solution #	Chemical 1	Chemical 2
1	13-100 vol.% phosphoric acid	0-2 *M* Cu oxide
2	0-56.25 vol.% phosphoric acid	6.25-100 vol.% ethylene glycol
3	10-90 vol.% phosphoric acid	0-0.5 *M* sodium tripolyphosphate
4	0-100 vol.% HEDP	0-30 vol.% phosphoric acid
5	0-100 vol.% ethylene glycol	1-5 *M* sodium chloride/ 1-4 *M* sodium nitrate
6	1-20 vol.% sulfuric acid	0-2.5 *M* sodium nitrate

Note: Phosphoric acid, 85 wt.% H_3PO_4; HEDP, 60 wt.% $C_2H_8O_7P_2$; sulfuric acid, 96.7 wt.%

3.1.1 Phosphoric Acid-Cu Oxide Solutions. Polarization curves were measured from phosphoric acid-copper oxide (CuO) solutions over the concentration range in which CuO can be dissolved. The solutions exhibited a nice blue color when the black CuO powder was well dissolved. All the measured curves had limiting current plateaus. The limiting current (i_L) data obtained from the measured polarization curves are plotted in Fig. 2.

It is shown that i_L (in range of 9-284 mA) decreases with increasing phosphoric acid and/or increasing CuO concentrations. The measured polarization curves show that E_L shifts to a higher potential and becomes narrower as the phosphoric acid concentration decreases in the range of 10-37%. E_L is about 0.5-1.7 V in the concentration range of 37-100% phosphoric acid and changes little as the concentrations of phosphoric acid and CuO change.

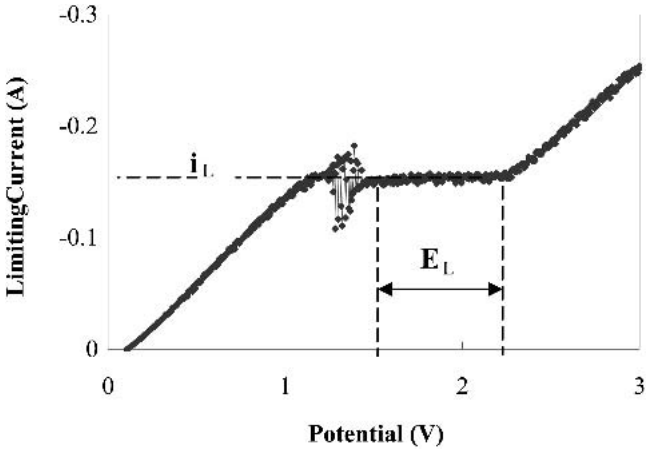

Fig. 1 Copper anodic polarization curve obtained from solution 54 vol.% phosphoric acid + 1.2 *M* Cu oxide with disk rotating speed 100 rpm and at room temperature

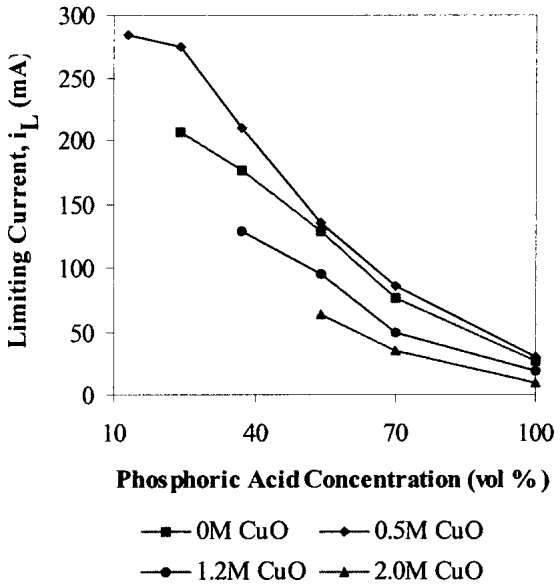

Fig. 2 Limiting current versus phosphoric acid concentration with different CuO concentrations

3.1.2 Phosphoric Acid-Ethylene Glycol Solutions. When polarization curves were examined as a function of concentration, limiting current plateaus only in those solutions where the phosphoric acid/ethylene glycol (EG) ratio is greater than 1:6. The i_L versus EG concentration is plotted in Fig. 3.

The curves indicate that adding EG into the phosphoric acid solutions decreases i_L (in the range of 10-77 mA). Moreover, EG led to lower values of i_L. Diluting the phosphoric acid-EG solutions with 25% water increased i_L. Further, diluting the solutions with 50% water decreased i_L. The measured polarization curves also indicated that values of E_L in range of 0.5-2.5 V shifted slightly to higher values of potential with increasing EG concentration or increasing dilution.

3.1.3 Phosphoric Acid-Sodium Tripolyphosphate Solutions. In the full concentration range of phosphoric acid-sodium tripolyphosphate ($Na_5P_3O_{10}$) solutions, polarization curves with limiting current plateaus were obtained from almost all the solutions. The i_L data are plotted in Fig. 4. It is shown that i_L (16-284 mA) decreases with increasing phosphoric acid and/or sodium tripolyphosphate concentrations. The measured polarization curves showed that sodium tripolyphosphate did not have obvious impact on E_L.

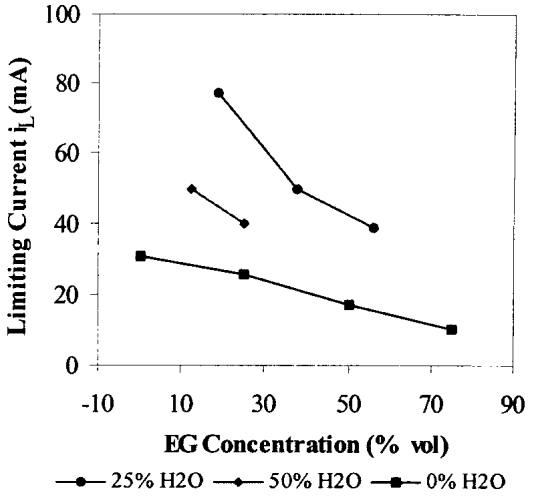

Fig. 3 Limiting current versus EG concentration with different H_2O concentrations

3.1.4 Hydroxyethylidenediphosphonic Acid-Phosphoric Acid Solutions. Limiting current plateaus appeared in all the polarization curves for the solutions investigated with i_L versus hydroxyethylidenediphosphonic acid (HEDP) concentration plotted in Fig. 5.[3] This plot shows that i_L (6-264 mA) decreases with increasing HEDP except at lower (<20% HEDP) concentrations and without phosphoric acid, in which case i_L increases with increasing HEDP concentration. The measured polarization curves also indicated that E_L is about 0.5-1.5 V for solutions of HEDP > 40%. For solutions of HEDP < 40%, decreasing the HEDP concentration shifts E_L to higher values and narrows E_L as well.

3.1.5 Ethylene Glycol-Sodium Chloride/Nitrate Solutions. The solubility of sodium chloride (NaCl) and sodium nitrate ($NaNO_3$) decreases with increasing EG concentration. Polarization curves were measured for EG-NaCl and EG-$NaNO_3$ solutions in their solubility range. There was no limiting current plateau in the polarization curves obtained from the EG-$NaNO_3$ solutions and EG solution with EG concentrations > 50%. The i_L data from polarization curves that exhibit limiting current plateaus are plotted in Fig. 6. It is seen that i_L (20-285 mA) increases with increasing NaCl concentration and decreases with increasing EG concentration.

All the polarization curves that exhibit limiting current plateaus have a wide range of E_L, about 2-4 V (4 V was the maximum potential scanned).

3.1.6 Sulfuric Acid-Sodium Nitrate Solutions. Polarization curves were measured for 1-20% sulfuric acid (H_2SO_4) with 0-2.5 *M* sodium nitrate ($NaNO_3$) solutions. The i_L data from polarization curves that exhibited limiting current plateaus are plotted in Fig. 7. From the figure, it can be seen that

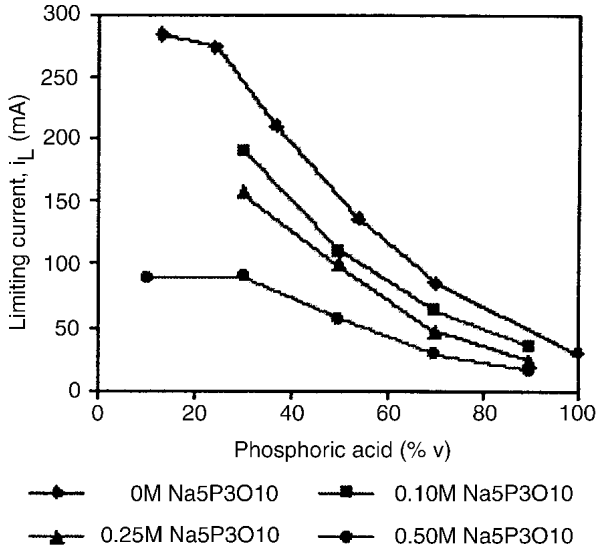

Fig. 4 Limiting current versus phosphoric acid concentration with different sodium tripolyphosphate concentrations

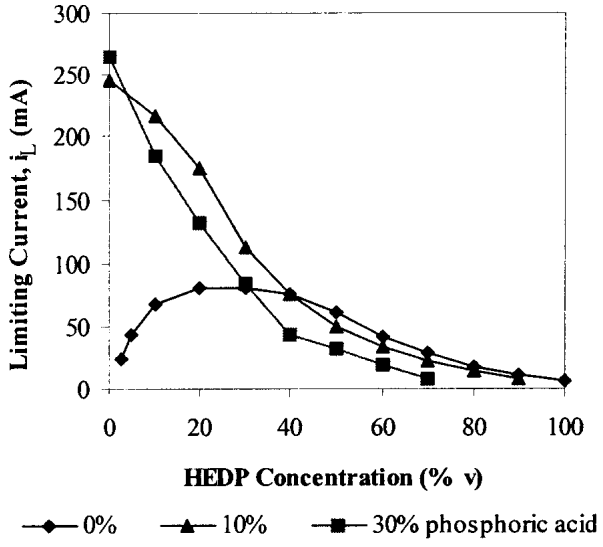

Fig. 5 Limiting current versus HEDP concentration with different phosphoric acid concentrations

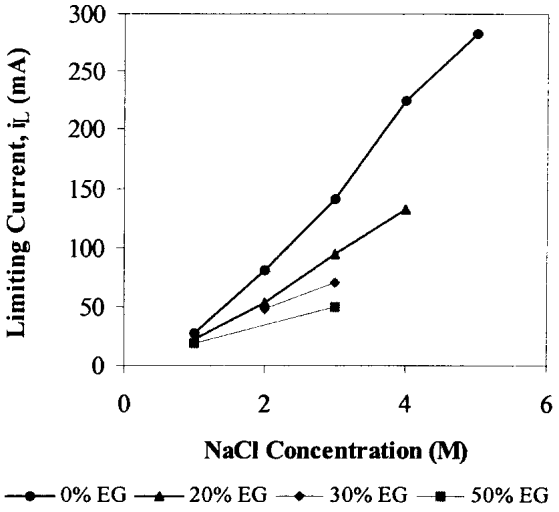

Fig. 6 Limiting current versus NaCl concentration with different EG concentrations

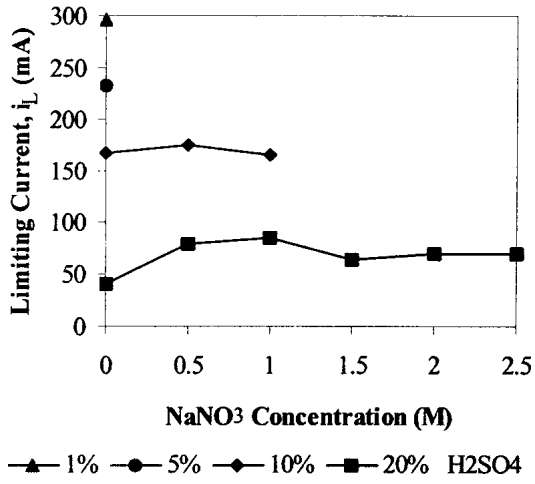

Fig. 7 Limiting current versus $NaNO_3$ concentration with different H_2SO_4 concentrations

i_L (in range of 41-296 mA) decreases with increasing H_2SO_4 concentration, while $NaNO_3$ concentration does not have significant effect to i_L. However, polarization curves showed that E_L (in the range of 1-4 V) was narrowed from 1-4 V to 3-4 V as the $NaNO_3$ concentration increased from 0.5 to 2.5 *M*.

3.2 ECP Results of Cu Bulk and Films

Based on the measured polarization curves, chosen solutions (as listed in Table 2) were used to investigate the influences of the electrolytes on the ECP effect of Cu bulk material. The ECP efficiency was evaluated with AFM. Typical AFM images of Cu disk surface before and after ECP are shown in Fig. 8. ECP data are listed in Table 2. From the data in Table 2 it can be seen that very good results for ECP efficiency of Cu bulk material can be achieved in solutions of phosphoric acid, HEDP, and phosphoric acid with additives of CuO, ethylene glycol, and sodium tripolyphosphate. However, Cu bulk ECP

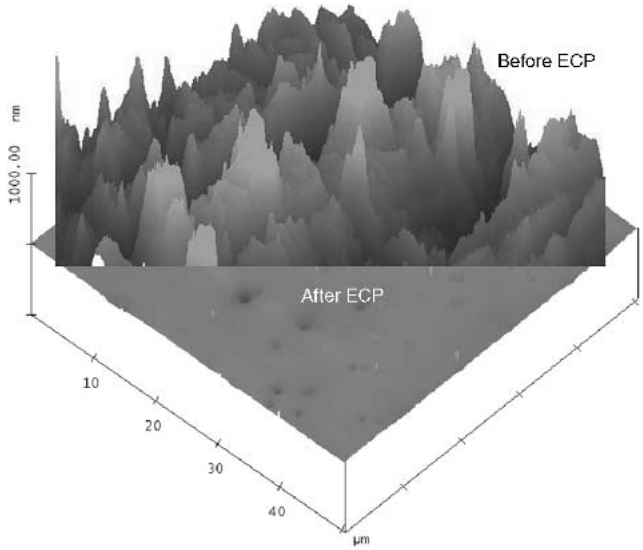

Fig. 8 AFM images of Cu disk surface before (R_a = 284 nm) and after ECP in 70% phosphoric acid + 15% EG solution (R_a = 6 nm)

Table 2 Summary of Cu Disk ECP Data

Solution	i_L, mA	R_d, μm/min	R_a, nm
30-100% phosphoric acid + 0-2 *M* CuO	20-200	0.44-4.4	5-29
70% phosphoric acid + 5-25% EG	14-50	0.3-1.1	5-8
70% phosphoric acid + 0.1-0.5 *M* $Na_5P_3O_{10}$	32-50	0.7-1.1	7-17
20-80% HEDP + 10-30% phosphoric acid	14-167	0.3-3.7	6-243
20-100% EG + 1-2 *M* NaCl	20-50	0.44-1.1	63-91
20% H_2SO_4 + 0-2 *M* $NaNO_3$	70-80	1.54-1.75	72-279

Note: phosphoric acid, 85 wt.%; HEDP, 60 wt.% $C_2H_8O_7P_2$

in an ethylene glycol-sodium chloride, sulfuric acid, and sulfuric acid-sodium nitrate solutions was not so good.

Among the electrolyte systems that can produce a good ECP effect, phosphoric acid and HEDP solutions were chosen to study the ECP effect of Cu film electroplated on deep trenched wafers. This choice was based on the knowledge from a previous study: (1) good ECP of Cu can be achieved in phosphoric acid (with or without additives) and HEDP solutions; (2) anodic layers formed during ECP process play a critical role;[2] and (3) the electrolyte solutions that can produce good ECP fall in two different groups:[1] (a) HEDP solutions, which form salt film on the Cu anode surface during ECP; and (b) solutions of phosphoric acid and phosphoric acid with additives, which do not form salt film on Cu anode surface during ECP.

SEM images of Cu film-silicon cross section before and after ECP in phosphoric acid and HEDP solutions, respectively, are shown in Fig. 9. A planar surface is obtained from ECP in HEDP solution. Nevertheless, the ECP in phosphoric acid was not as good. Bumps over dense structures were left behind after ECP. An interpretation of the above ECP results are presented after the discussion of ECP mechanisms in the next section.

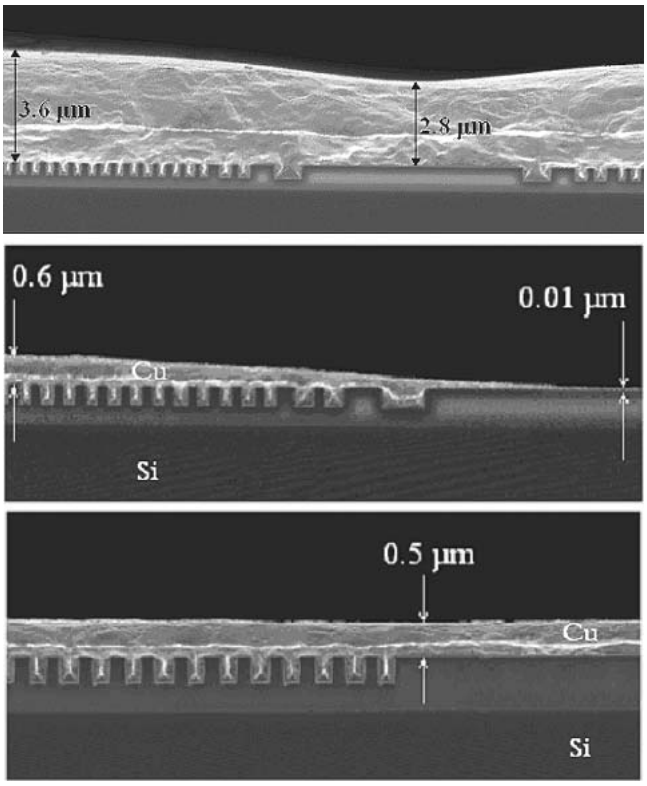

Fig. 9 SEM images of Cu film-silicon cross section **(a)** before and **(b)** after ECP in phosphoric acid and **(c)** HEDP solutions

3.3 Mechanisms of Electropolishing

Electrochemical planarization, electrochemical polishing, or electropolishing is abbreviated as ECP and can be achieved under ohmic control or mass transport control.[2] Under ohmic control, the leveling effect of surface roughness (ohmic leveling) is realized due to the protruding areas having a higher current density (J) than the recesses. Under mass transport control, characterized by a limiting current plateau in the anodic polarization curves and a straight line on the Levich plot,[4-6] mass transport is the slowest among all the processes (such as anodic reaction). Thus, a concentration gradient of the mass transport limiting species is developed in the anode boundary layer as determined by hydrokinetics.[4] In some cases, a resistive salt film forms on the anode surface in the mass transport limiting species concentrated layer.[1,7,8] Such anode layers suppress crystallographic etching[2,9-11] and facilitate surface smoothing through migration and diffusion smoothing effects.

3.4 Ohmic Leveling

On a rough anode surface as shown in Fig. 10, the current densities at a protruding point P and a recessed point Q are different due to the distances between P and Q to cathode (thus, different electrical resistance from the solution). Accordingly, there is a difference in the anodic dissolution rate (R_d) between P and Q, which can be expressed as[1]

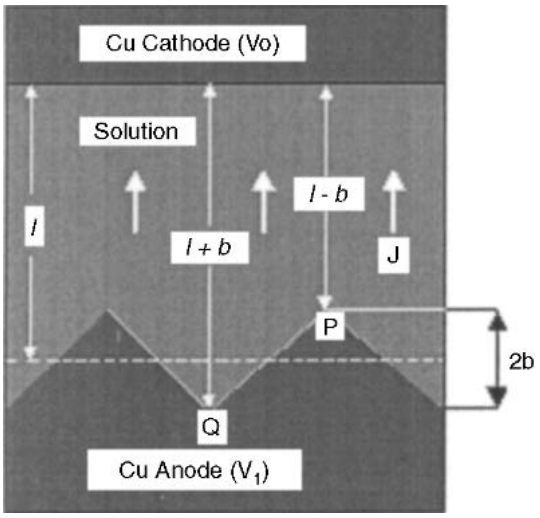

Fig. 10 Schematic illustration of an ECP cell with rough anode surface

$$\Delta R_d = R_d\,(\mathrm{P}) - R_d\,(\mathrm{Q}) = f\frac{2b}{\rho_e(l^2 - b^2)} \qquad \text{(Eq 1)}$$

where $f = MV/nFd$, ρ_e is the resistivity of the electrolyte solution, M is the atomic weight (63.5 g for Cu), and d is the density of the anode material (8.96 g/cm^3 for Cu), n (2 for Cu $- 2e \rightarrow Cu^{2+}$ reaction) is the number of electrons transferred in the oxidation reaction, and F (= 96 485 C) is the Faraday constant.

From Eq 1 the leveling effect due to ohmic resistance can be produced if the amplitude of anode surface fluctuation (b) is relatively large compared with interelectrode distance (l). This leveling effect is termed "ohmic leveling." Under general ECP conditions, ohmic leveling is negligible.[1]

However, under mass transport control, if an anode layer is formed under certain hydrokinetic conditions and has a macroprofile, as shown in Fig. 11, then ohmic leveling can be conspicuous. Due to forced convection, ion motion in a solution is much faster than in the anode layer. In other words, the anode layer determines the current density, and Eq 1 can be written as

$$\Delta R_d = R_d\,(\mathrm{P}) - R_d\,(\mathrm{Q}) = f\frac{\delta_2 - \delta_1}{\rho_f \delta_1 \delta_2} \qquad \text{(Eq 2)}$$

where ρ_f is the resistance of the anode layer. Under normal ECP conditions,[1] ΔR_d can be seven times higher than the average anode dissolution rate. Therefore, in this case the ohmic leveling effect is conspicuous.

3.5 Migration Smoothing

The motion of ions under the influence of an electric field is called migration. Cu^{2+} migration occurs in the anode layer. Outside this layer, forced convection dominates. Previous studies[1,4] indicate that the electric field distribution on a rough surface depends on the surface profile. Figure 12 shows the normal electrical field (E_n) distribution along a sinusoidal anode surface obtained by computer simulation with boundary

element simulation software. The shape of the E_n-X curve is conformal to the surface profile. That is, the amplitude of normal electric field at peak point P, E_n(P), is larger than that at valley point Q, E_n(Q). The direction of the electric field varies with X. E_n(P) and E_n(Q) point perpendicular to the cathode. Hence, the Cu^{2+} (produced by anodic reaction) at P sees a larger force applied by the electric field and moves toward the cathode at a faster rate than the Cu^{2+} at Q. Therefore, the Cu dissolution rate at the peak area (P) is expected to be greater than that in the valley area (Q), which results in surface leveling, or smoothing (i.e., "migration smoothing").

The simulation data[1,4] show that the amplitude difference (ΔE_n) of the normal electrical field between peak (P) and valley (Q) depends on the frequency of the anode surface profile (sine wave), as shown in Fig. 13. A shorter wave (higher frequency) has greater ΔE_n than a longer wave (lower frequency). Therefore, the migration smoothing effect, driven by ΔE_n, approaches a sine wave profile involving the greatest wavelength of the original pattern since shorter waves disappear faster than the longer waves.

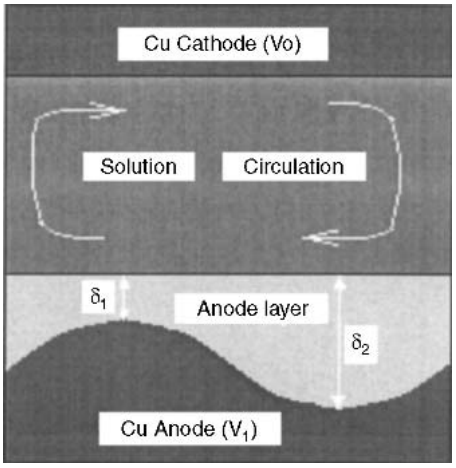

Fig. 11 Schematic illustration of an ECP cell with nonconformal anode layer

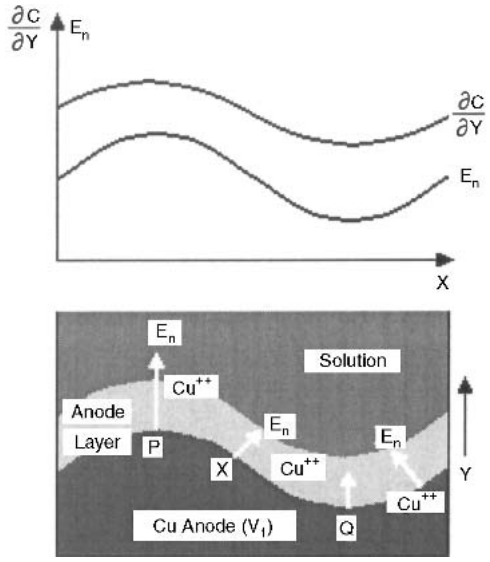

Fig. 12 Schematic illustration of the distribution of normal electric field on a sinusoidal anode surface

3.6 Diffusion Smoothing

Under mass transport control, a concentration gradient of the mass transport limiting species is developed in the anode boundary layer. Figure 14 shows the concentration profile from the anode surface through the anode layer to the bulk solution. In the graph, C_b is the concentration in the bulk solution while δ_c is the thickness of the anode layer. Wagner[12] calculated the distribution of the concentration gradient along a sinusoidal anode surface using Fick's diffusion law and boundary conditions, assuming mass transport control, acceptor mechanism, and $b \ll a$ and $a \ll \delta_c$.

The concentration gradient ($\partial C/\partial Y$) at the anode surface is given by

$$\left(\frac{\partial C}{\partial Y}\right)_{y=b\sin\left(\frac{2\pi}{a}x\right)} = B\left[1 + 2\pi\frac{b}{a}\sin\left(\frac{2\pi}{a}x\right)\right] \quad \text{(Eq 3)}$$

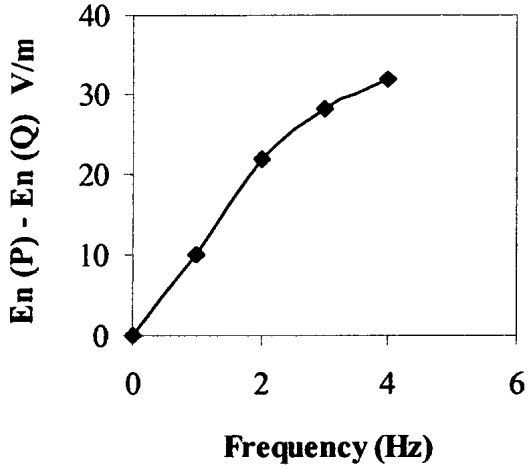

Fig. 13 Amplitude of normal electric field at peak (P) and valley (Q) points of a sinusoidal anode surface

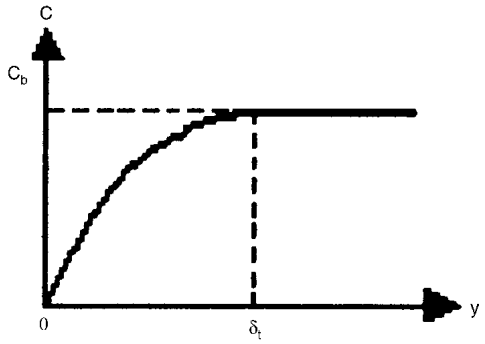

Fig. 14 Acceptor concentration as a function of distance from the anode surface

This is illustrated in Fig. 12. In the above equation, B is the average value of concentration gradient at the anode surface, with a and b the wavelength and amplitude of the sinusoidal surface profile, respectively.

From Fig. 12 the concentration gradient at the peak is higher than that in the valley, i.e., $(\partial C/\partial Y)_P > (\partial C/\partial Y)_Q$. Similar to migration smoothing, which is driven by electric field difference (ΔE_n) between P and Q, "diffusion smoothing" is driven by the difference of concentration gradient between P and Q. Wagner further calculated the dissolution rate of Cu at the Cu anode surface[12]

$$R_d = C\left(2\pi\frac{b}{a}\right)\sin\left(\frac{2\pi}{a}x\right) \quad \text{(Eq 4)}$$

Equation 4 indicates that the dissolution rate versus location x has the same shape as the geometric profile of the anode surface. That is, R_d at the peak is greater than that at the valley of the anode surface. Equation 4 also suggests that R_d increases with decreasing wavelength a. In other words, "microroughness" will disappear more rapidly than "macroroughness." Therefore, ECP due to the diffusion smoothing mechanism approaches a sine wave profile involving the greatest wavelength of the original pattern.

From the above discussions, it is impossible to get an absolute flat surface through migration smoothing and diffusion smoothing mechanisms. However, the situation can be improved if the anode layer (the concentration gradient layer or an electrical resistive salt film) has a macroprofile. In this case, the migration and/or diffusion distance of the mass transport limiting species at peak points is shorter than that at the valley points (Fig. 11).

4. Interpretation of ECP Results

According to the above discussions, better ECP can be achieved in the case of sharper geometrical profiles, due to migration or diffusion smoothing mechanisms. This explains why very good ECP efficiency was obtained from all the solutions with Cu disks, which have sharp surface profiles (Fig. 8). Yet ECP efficiency is largely reduced in those cases of gentle surface profiles, such as the surface features of patterned electroplated (EP) Cu films on a wafer, as shown in Fig. 15. On the surface of EP Cu films, large pads and wide stripes were about 0.2-0.5 μm higher than the flat areas and had gentle geometrical changes, especially after a period of ECP process. Therefore, due to gentle surface undulation, and/or due to a lack of ion migration mechanism (e.g., water molecules instead of Cu ions as the mass transport control species in case of Cu ECP in phosphoric acid and phosphoric acid + CuO[1,6]), the dissolution rates at protruding and recessed areas were not very different in phosphoric acid. Therefore, the original surface profile changed little, as shown in Fig. 9.

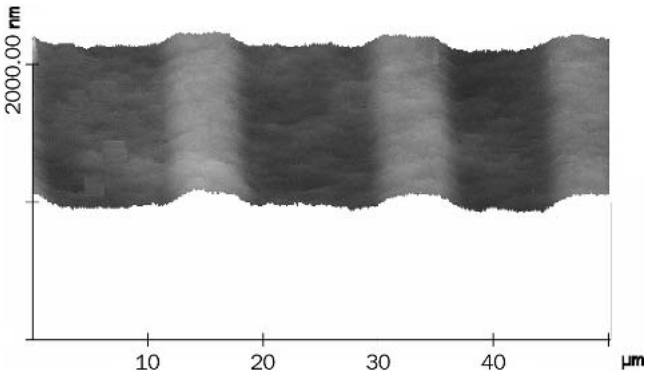

Fig. 15 AFM image of Cu film electroplated on patterned silicon wafer

However, when an electrically resistive salt film with a macroprofile formed on the anode surface and with the mass transport limiting species being Cu^{2+},[1] all three ECP mechanisms take effect. Therefore, a good ECP efficiency was achieved, even though the surface had a gentle geometric profile. This explains why good planarization of Cu films plated on a trenched wafer was obtained (Fig. 9) in HEDP solution.

5. Summary and Optimal Conditions for ECP of Cu Film Electroplated on Patterned Silicon Wafer

Very good electropolishing results (surface mean roughness R_a < 10 nm) of bulk Cu were obtained in solutions of phosphoric acid, HEDP, and phosphoric acid with additives CuO, ethylene glycol, and sodium tripolyphosphate.

Electropolishing of EP Cu films on patterned silicon wafers is more difficult. Gently protruding areas were not planarized by the ECP process with phosphoric acid while a good planarization was obtained in HEDP solutions, where salt films formed on the anode surface.[1] A salt film with macroprofile on the anode may benefit from ohmic leveling, migration smoothing, and diffusion smoothing effects.

If the surface layer has a microprofile, the ECP effect depends on the sharpness of the surface undulation. Therefore, the surface profile of the anode layer is crucial to ECP of Cu films on patterned silicon wafers. The surface profile of anode layer depends on the viscosity of the layer and the solution, and the convection conditions of the electrolyte.

Ideal conditions for ECP of Cu films electroplated on patterned silicon wafers are:

- The polarization curve has a wide and level limiting current plateau with relatively low limiting current (e.g., 10 mA).[4]
- Formation of an electrically resistive salt film on the anode surface during ECP resulting in a nonconformal surface profile of the Cu film to be planarized (i.e., macroprofile).
- ECP is processed with potential control.
- Good circulation of the electrolyte solution to ensure uniform ECP over large area of anode surface.
- Design of the ECP cell to prevent hydrogen bubbles from reaching the anode surface while using parallel and vertical electrodes.
- An extremely close interelectrode distance facilitates ohmic leveling effect; however, this also allows hydrogen bubbles to more easily reach the anode surface.

The above conditions depend mainly on the electrolytes and their concentration, as well as temperature. Further research is needed to explore the ideal electrolyte solutions and ECP parameters corresponding to the above optimal conditions.

Acknowledgments

The authors wish to acknowledge Ms. Nancy Zelick at Intel Corporation and Mr. Jay Jordan at FEI Company for their assistance in preparing wafer samples and their SEM images.

References

1. J. Huo, R. Solanki, and J. McAndrew: "Study of Anodic Layers and Their Effects on Electropolishing of Bulk and Electroplated Films of Copper," *J. Appl. Electrochem.* 2003, *34,* pp. 305-14.
2. D. Landolt: "Review Article Fundamental Aspects of Electropolishing," *Electrochim. Acta,* 1987, *32,* pp. 1-11.
3. J. Huo, R. Solanki, and J. McAndrew: "Electrochemical Polishing of Copper for Microelectronic Applications," *Surf. Eng.,* 2003, *19,* pp. 11-16.
4. J. Huo: "Electrochemical Planarization of Copper for Microelectronic Application," Doctoral Dissertation, OGI of Science and Engineering, Oregon Health and Science University, Beaverton, OR, 2003.
5. A.J. Bard and L.R. Faulkner: *Electrochemical Methods Fundamentals and Applications,* 2nd ed., John Wiley & Sons, New York, 2001, p. 339.
6. R. Vidal and A.C. West: "Copper Electropolishing in Concentrated Phosphoric Acid," *J. Electrochem. Soc.,* 1995, *142,* pp. 2682-94.
7. R. Alkire and A. Cangellari: "Effect of Benzotriazole on Dissolution of Copper in Presence of Fluid Flow," *J. Electrochem. Soc.,* 1989, *136,* pp. 913-19.
8. C. Serre, S. Barret, and R. Herino: "Characterization of the Electropolishing Layer During Anodic Etching of p-Type Silicon in Aqueous HF Solutions," *J. Electrochem. Soc.,* 1994, *141,* pp. 2049-53.
9. R. Soutebin and D. Landolt: "Anodic Leveling Under Secondary and Tertiary Current Distribution Conditions," *J. Electrochem. Soc.,* 1982, *129,* pp. 946-53.
10. H. Abrams and C.L. Mantell: "Electrolytic Polishing of Copper and Nickel Silver," *Electrochem. Tech.,* 1967, *5,* pp. 287-92.
11. M. Matlosz, S. Magaino, and D. Landolt: "Impedance Analysis of a Model Mechanism for Acceptor-Limited Electropolishing," *J. Electrochem. Soc.,* 1994, *141,* pp. 410-18.
12. C. Wagner: "Contribution to the Theory of Electropolishing," *J. Electrochem. Soc.,* 1954, *101,* pp. 225-28.